19 Sep 2016

Comparison Of Mixed-mode S-parameters In Weak And Strong Coupled Differential Pairs

Marina Koledintseva
Missouri University of Science and Technology, marinak@mst.edu

Tracey Vincent

Recommended Citation

M. Koledintseva and T. Vincent, "Comparison Of Mixed-mode S-parameters In Weak And Strong Coupled Differential Pairs," *IEEE International Symposium on Electromagnetic Compatibility*, pp. 610 - 615, article no. 7571718, Institute of Electrical and Electronics Engineers, Sep 2016.
The definitive version is available at https://doi.org/10.1109/ISEMC.2016.7571718

Comparison of Mixed-mode S-parameters in Weak and Strong Coupled Differential Pairs

Marina Koledintseva [*1] and Tracey Vincent[#2]

[*] *Oracle, Menlo Park, CA, USA,* [#]*CST of America, Framingham, MA, USA*

[1]koledintseva@gmail.org, [2]tracey.vincent@cst.com

Abstract**—** In this paper, it is studied how the rate of coupling (weak vs. strong) in edge-coupled differential transmission lines on a printed circuit board (PCB) affects frequency behavior of mixed-mode S-parameters. This is important for signal integrity (SI), and also may be useful from electromagnetic compatibility (EMC) point of view, since the enhancement of mode conversion (from common-mode to differential mode, and vice versa) may result in common-mode noise in high-speed digital electronics. Slightly imbalanced in length microstrip and stripline differential pairs are considered. The study is done using full-wave numerical electromagnetic simulations.Various technological features are modeled in this work: rectangular vs. trapezoid shape of a signal trace cross-section; copper foil roughness; solder mask over microstrip lines; and presence of an epoxy-resin "pocket" (EP) between the stripline traces (dielectric properties of the EP are different from the homogenized parameters of the ambient dielectric where these traces are embedded).

I. Introduction

Study of hybrid, or mixed-mode S-parameters (S_{dd}, S_{cc}, S_{cd}, and S_{dc}) of differential transmission lines on printed circuit boards (PCBs) is important for both signal integrity (SI) and electromagnetic compatibility (EMC) [1]. The quality of the differential mode (DM), which determines SI, is associated with the frequency dispersion and loss on the line. The common mode (CM) is inevitable on differential pairs. It may become a source of unwanted electromagnetic interference (EMI), especially in the I/O connector areas at multigigabit per second data rates, if shielding is compromised. Imbalanced differential microstrip lines on the top (or bottom) layers of a PCB may be the direct source of EMI. Imbalanced differential striplines on the inner layers of a PCB may also cause unwanted radiation, if the lines come close enough to an edge of the board. In addition to DM and CM, the imbalanced differential pairs produce mode conversion: the conversion from CM to DM affects SI, while the conversion from DM to CM may contribute to EMC/EMI problems. The higher the imbalance, the more mode conversion is produced; that is why in the high-speed digital designs there are restrictions on imbalances, inlcuding length difference in a pair.

The imbalances in edge-coupled microstrip lines with the bend-type discontinuity, i.e., length difference, were studied numerically and experimentally in [2]. There were two types of coupling between lines: strong coupling ($h>s$) and weak (loose) coupling ($h<s$), where h is the thickness of the substrate, and s is the edge-to-edge separation of the traces. The differential impedance in both cases was 100Ω over the frequency range below 10 GHz. It was shown that the weak coupling is preferable from both SI and EMI points of view.

Indeed, weakly coupled differential pairs are widely used in high-speed PCB designs [3]. However, for space saving, strong (or tight) coupling of signal traces may be desirable. But pusing differential traces close to each other necessitates a trace width reduction, which may increase losses at the higher frequencies and affect eye diagram closure.

The objective of the work is to find out how the rate of coupling (weak vs. strong) between two lines in a differential pair affects mixed-mode S-parameters, if the lines are at least slightly imbalanced. Also, it is important to take into account frequency dispersive nature of a PCB dielectric and various technological features, such as copper foil roughness, solder mask on microstrip lines, and trapezoid shape of of signal trace cross-sections. None of these factors were considered in [2]. However, they were implemented in [4], where edge-coupled microstrip differential pairs, straight and bent, with different length imbalances were modeled numerically, but only weakly-coupled cases. In this work, both weak- and strong-coupled cases (microstrip and stripline) with various technological effects taken into account are studied.

II. Numerical Electromagnetic Model Description

The following cases are modeled in this work:

I. Microstrip edge-coupled differential pairs:

- weak and strong coupled;
- rectangular 90^0 traces and trapezoid traces (60^0 and 45^0);
- with/without copper foil roughness;
- with/without solder mask.

II. Stripline edge-coupled differential pairs:

- weak and strong coupled;
- rectangular 90^0 traces and trapezoid traces (60^0 and 45^0);
- with/without copper foil roughness;
- with/without epoxy-resin "pocket".

All the structures in this work are modeled using CST STUDIO SUITE™ [5]. The cross-sectional view of the microstrip structure is shown in Fig. 1, and of the stripline structure is in Fig. 2. Herein, the imbalance is introduced by the different physical lengths of the signal traces. Copper foil roughness is modeled as effective roughness dielectric (ERD) [6]. In addition, in stripline case, the effect of an epoxy-resin "pocket" (EP) between the traces is studied. The dielectric properties of this "pocket" are different from the homogenized parameters of the dielectric matrix where these traces are embedded. Therefore there are different conditions for propagating CM and DM, since the electromagnetic fields of the DM are mainly concentrated between the traces, while the

978-1-5090-1442-2/16/$31.00 ©2016 IEEE

CM fields are mainly between the traces as a whole and the ground planes.

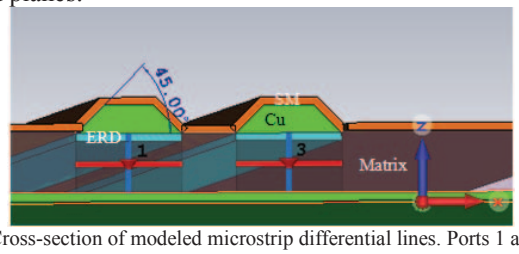

Fig. 1. Cross-section of modeled microstrip differential lines. Ports 1 and 3 are on the one end, and 2 and 4 on the other.

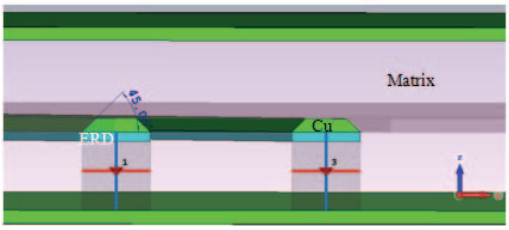

Fig. 2. Differential striplines with trapezoid-shape traces embedded in the ambient dielectric matrix; ERD is shown.

The lengths of the straight traces are first taken as L_1=80 mm and L_2=80.127 mm, i.e. there is a typical for the PCB design 5-mil length imbalance. The lines are equidistant with respect to the edges of the PCB in the model: the distances between the edge of each trace to the nearest PCB edge are h_{t1}=h_{t2}=2 mm. In all the models, Ports 1 and 3 are on one side of the board, and Ports 3 and 4 are on the other. The cross-sections of all the modeled structures, both weak- and strong-coupled, provide the 100-Ω differential impedance. The signal traces are either rectangular (90^0), or trapezoid (60^0 or 45^0).

In all the cases, the ambient dielectric matrix was taken as the dispersive Megtron 6 [6]. The copper foil roughness is substituted by an ERD layer, corresponding to STD foil. STD foil is smooth on the "oxide" (drum) side, and is rough on the "foil" (matte) side. ERD layer is placed only on the "foil" side; its thickness is T_r=2A_r=12.4 μm, and dielectric parameters are ε_{rough}'=12; tanδ_{rough}=0.17 [7]. The ground planes (GPs) in all the models have the same thickness, t_{gp}=0.0175 mm. The surface roughness on the GPs is not modelled: the current density on the ground planes is much lower than that on the signal traces.

A. *Microstrip Models Setup*

The thickness of copper on the microstrip line is t_{ms}=0.0462 mm, and the dielectric substrate height is h=0.1 mm. In the weak-coupled lines, the width of each signal trace is w_t= 0.203 mm, and separation distance is s_t=0.18 mm. In the strong-coupled case, the trace width is w_t=0.1735 mm, and trace spacing is s_t=0.0889 mm. The typical solder mask thickness is t_{sm}=0.5mil=0.0127 mm, and the constant dielectric parameters over the frequency range of interest are taken as ε'_{sm}=4.5 and tanδ_{sm}=0.05 as in [4].

B. *Stripline Models Setup*

The modeled striplines are symmetrical, with the distance between the ground planes of h=0.22 mm. Copper thickness on the traces and on the ground planes is t_{sl}=t_{gp}=0.0175 mm. In the weak-coupled lines, the width of each trace is w_t=0.087 mm and the trace spacing is s_t=0.275 mm. In the strong-coupled case, w_t=0.104 mm, and is s_t=0.1 mm.

In some cases, the "epoxy pocket" (EP) region between the traces is modeled (see Fig. 3). It is taken as pure non-dispersive epoxy resin, with ε'_{epoxy}=3.0 and tanδ_{epoxy}=0.07 at 10 GHz; these parameters are different from those of the ambient dielectric matrix. ERD on the sides of the traces may also affect mixed-mode S-parameters.

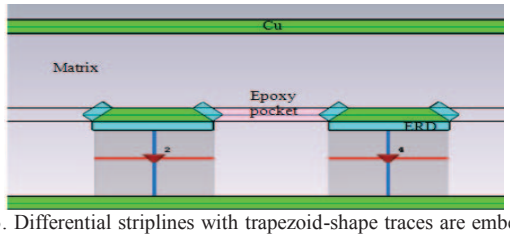

Fig. 3. Differential striplines with trapezoid-shape traces are embedded in the ambient dielectric matrix; ERD is on the sides of the traces and under the traces, and the epoxy-resin "pocket" is between the traces.

III. Numerical Modeling Results for Microstrips

The CST [6] models were run in both time-domain (FIT solver) and frequency domain. Since the results of computations agreed well within a fraction of dB over the entire frequency range, later FIT solver was used because it is significantly faster. The computational results at 10 GHz and 40 GHz for rectangular/trapezoid traces and weak/strong coupling are summarized in Table I. The slopes of the linearized frequency dependences (in dB/GHz) are also calculated. They show how fast mixed-mode parameters decay with frequency. Some results are plotted in Figs. 4-9. These data are for 80-mm/80.127-mm imbalanced microstrips only, but can be normalized by length.

A. *Weak and Strong Coupling Effects for Rectangular Traces*

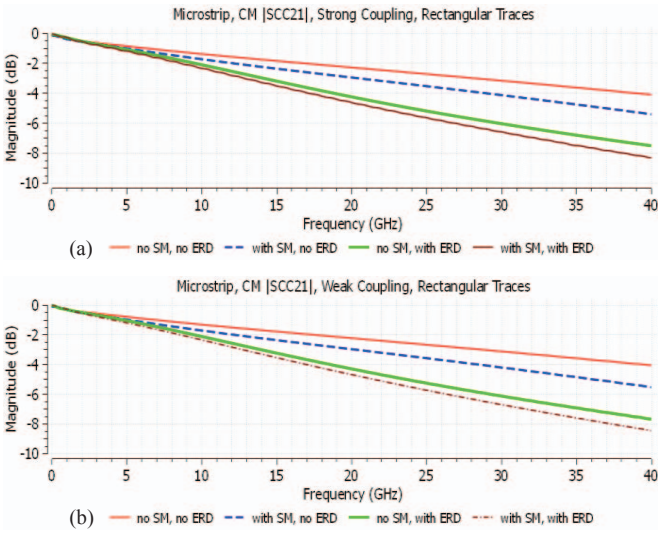

Fig. 4. CM ($|S_{cc21}|$) in strong (a) and weak (b) coupling

The insertion loss (IL) curves for CM in weak- and strong-coupled lines with rectangular traces, with/ without solder

mask, and with/ without ERD are presented in Fig. 4. IL for CM is slightly larger for the strong coupling at the higher frequencies of 35-40 GHz; but there is not much difference at the lower frequencies. The IL curves for the corresponding DM are presented in Fig. 5. It is seen that the loss for DM is slightly smaller than for CM in both weak- and strong-coupled cases. At the higher frequencies, loss in weak-coupled lines is less than in the strong-coupled ones. In all the cases, both SM and ERD cause the larger loss, which is an obvious result.

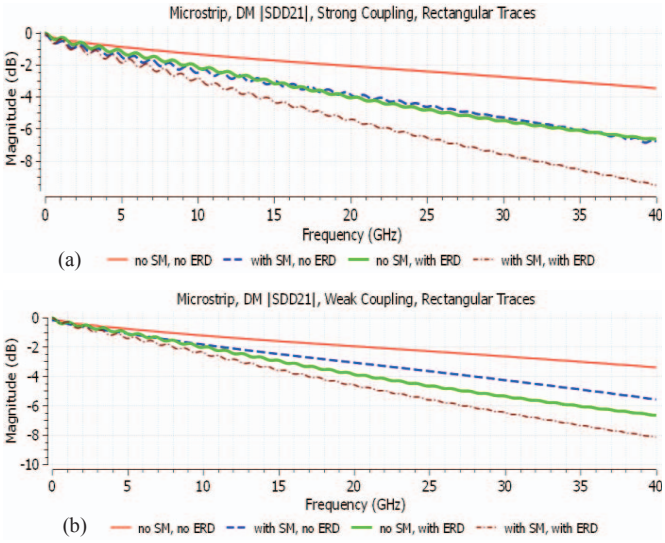

Fig. 5. DM ($|S_{dd21}|$) in strong (a) and weak (b) coupling

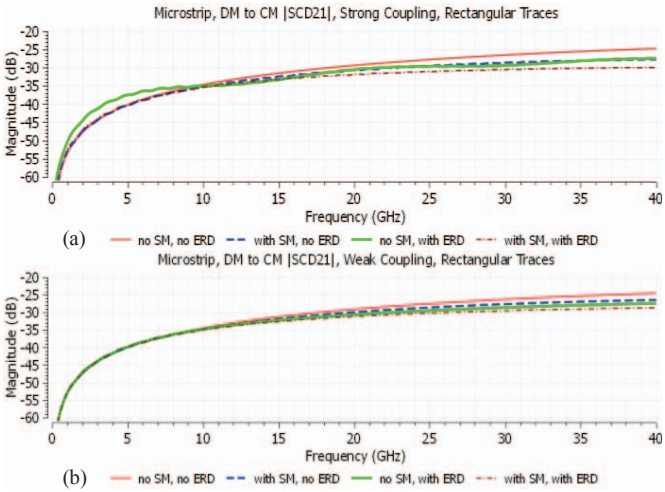

Fig. 6. Mode conversion ($|S_{cd21}|=|S_{dc21}|$) in strong (a) and weak (b) coupling

Fig. 6 shows that the coupling rate almost does not affect mode conversion. However, at the lower frequencies (herein, f<10 GHz), the ERD may slightly enhance mode conversion in the strong-coupled case. This is because the rougher surface is beneath the traces, where CM propagates, and at the strong coupling, the field is more concentrated between the traces than between the traces and the ground. With the less intense CM fields, a subtle effect of foil roughness becomes more significant, causing the bigger difference in the mode conversion.

TABLE I.
MIXED-MODE S-PARAMETERS AND SLOPES FOR MICROSTRIP DIFFERENTIAL PAIRS WITH 5-MIL (0.127 MM) IMBALANCE

Case	Parameter, dB	10 GHz	40 GHz	Slope, dB/GHz	Technological effects modeled
Strong coupling, rect. traces	|Scc21|	-1.378	-4.096	-0.0906	No SM, no ERD
		-1.759	-5.389	-0.1210	With SM, no ERD
		-2.092	-7.504	-0.1804	No SM, with ERD
		-2.316	-8.307	-0.1997	With SM & ERD
	|Sdd21|	-1.342	-3.466	-0.0708	No SM, no ERD
		-2.221	-6.739	-0.1386	With SM, no ERD
		-2.148	-6.639	-0.1497	No SM, with ERD
		-2.856	-9.528	-0.2224	With SM & ERD
	|Scd21|	-34.67	-24.75	+0.3307	No SM, no ERD
		-34.70	-27.47	+0.2410	With SM, no ERD
		-34.70	-27.46	+0.2413	No SM, with ERD
		-35.29	-29.98	+0.1770	With SM & ERD
Weak coupling, rect. traces	|Scc21|	-1.330	-4.075	-0.0915	No SM, no ERD
		-1.732	-5.556	-0.1247	With SM, no ERD
		-2.130	-7.695	-0.1843	No SM, with ERD
		-2.357	-8.473	-0.2033	With SM & ERD
	|Sdd21|	-1.230	-3.397	-0.0722	No SM, no ERD
		-1.842	-5.580	-0.1246	With SM, no ERD
		-2.031	-6.661	-0.1543	No SM, with ERD
		-2.391	-8.158	-0.1922	With SM & ERD
	|Scd21|	-34.44	-24.56	+0.3293	No SM, no ERD
		-34.43	-26.48	+0.2650	With SM, no ERD
		-34.50	-27.45	+0.2350	No SM, with ERD
		-34.94	-28.73	+0.2070	With SM & ERD
Strong coupling, 60^0 traces	|Scc21|	-1.499	-4.293	-0.0931	No SM, no ERD
		-1.874	-5.804	-0.1310	With SM, no ERD
		-2.311	-7.974	-0.1888	No SM, with ERD
		-2.515	-8.732	-0.2072	With SM & ERD
	|Sdd21|	-1.432	-3.779	-0.0782	No SM, no ERD
		-2.381	-7.155	-0.1591	With SM, no ERD
		-2.381	-7.447	-0.1689	No SM, with ERD
		-2.971	-9.869	-0.2300	With SM & ERD
	|Scd21|	-34.86	-25.01	+0.3283	No SM, no ERD
		-35.13	-27.81	+0.2440	With SM, no ERD
		-35.34	-28.37	+0.2323	No SM, with ERD
		-35.53	-30.44	+0.1697	With SM & ERD
Weak coupling, 60^0 traces	|Scc21|	-1.448	-4.329	-0.0960	No SM, no ERD
		-1.448	-5.758	-0.1437	With SM, no ERD
		-2.243	-8.013	-0.1923	No SM, with ERD
		-2.496	-8.849	-0.2177	With SM & ERD
	|Sdd21|	-1.359	-3.730	-0.0790	No SM, no ERD
		-1.917	-5.784	-0.1289	With SM, no ERD
		-2.114	-7.150	-0.1679	No SM, with ERD
		-2.554	-8.648	-0.2031	With SM & ERD
	|Scd21|	-34.61	-24.94	+0.3223	No SM, no ERD
		-34.71	-26.71	+0.2667	With SM, no ERD
		-34.90	-27.73	+0.2390	No SM, with ERD
		-35.09	-29.19	+0.1967	With SM& ERD
Strong coupling, 45^0 traces	|Scc21|	-1.514	-4.315	-0.0934	No SM, no ERD
		-1.878	-5.846	-0.1323	With SM, no ERD
		-2.347	-8.066	-0.1906	No SM, with ERD
		-2.542	-8.795	-0.2084	With SM & ERD
	|Sdd21|	-1.408	-3.770	-0.0787	No SM, no ERD
		-2.393	-7.142	-0.1583	With SM, no ERD
		-2.393	-7.672	-0.1760	No SM, with ERD
		-3.047	-10.101	-0.2351	With SM & ERD
	|Scd21|	-34.65	-24.960	+0.3230	No SM, no ERD
		-35.051	-27.851	+0.2400	With SM, no ERD
		-35.052	-28.582	+0.2157	No SM, with ERD
		-35.560	-30.622	+0.1647	With SM & ERD
Weak coupling, 45^0 traces	|Scc21|	-1.417	-4.295	-0.0959	No SM, no ERD
		-1.842	-5.771	-0.1310	With SM, no ERD
		-2.261	-8.096	-0.1945	No SM, with ERD
		-2.522	-8.948	-0.2142	With SM & ERD
	|Sdd21|	-1.352	-3.709	-0.0786	No SM, no ERD
		-1.938	-5.874	-0.1312	With SM, no ERD
		-2.129	-7.300	-0.1724	No SM, with ERD
		-2.615	-8.800	-0.2062	With SM & ERD
	|Scd21|	-31.180	-24.150	+0.2343	No SM, no ERD
		-34.431	-26.761	+0.2557	With SM, no ERD
		-34.432	-27.852	+0.2193	No SM, with ERD
		-35.121	-29.31	+0.1937	With SM & ERD

B. *Weak and Strong Coupling Effects for Trapezoid Traces*

Similar effects, as described above, are observed for the trapezoid cross-sections. Figs. 7-9 show the results for 45^0 traces. It is seen that weak coupling is preferable for less DM loss. The 45^0 traces result in slightly higher loss for DM than the 60^0 and 90^0 traces, as is seen from Table I.

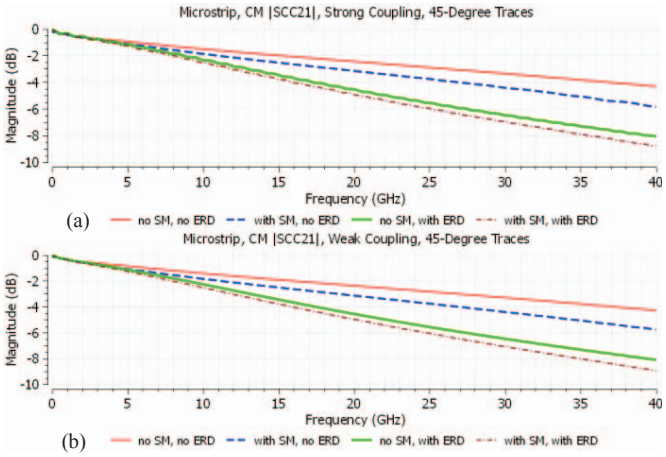

Fig. 7. CM ($|S_{cc21}|$) in strong (a) and weak (b) coupling

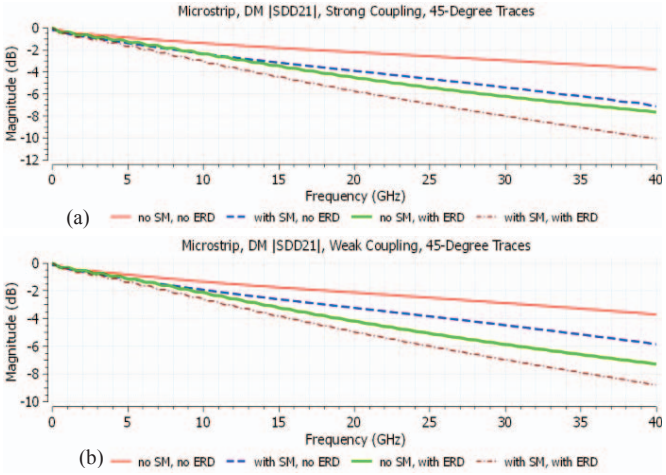

Fig. 8. DM ($|S_{dd21}|$) in strong (a) and weak (b) coupling

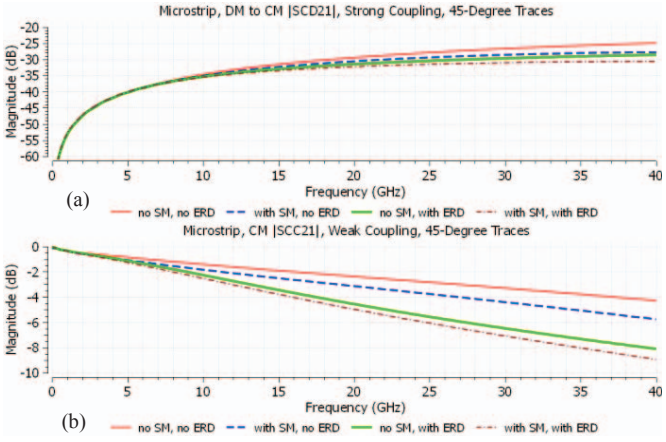

Fig. 9. Mode conversion ($|S_{cd21}|=|S_{dc21}|$) in strong (a) and weak (b) coupling

Mode conversion (Fig. 9) is slightly larger in the weak-coupled case for trapezoid traces, but no enhancement due to ERD is observed. This is because of the more inhomogeneous field between the trapezoid traces as compared to the rectangular ones. The 60^0 traces give intermediate results between the 90^0 and 45^0 cases (see Table I).

IV. Numerical Modeling Results for Striplines

Only FIT solver was used to model differential stripline pairs, since time-domain simulations are much faster than frequency domain over the wide frequency range. The modeling results for stripline differential pairs are shown in Figs. 10-14 and also summarized in Table II.

TABLE II.
MIXED-MODE S-PARAMETERS AND SLOPES FOR STRIPLINE DIFFERENTIAL PAIRS WITH 5-MIL (0.127 MM) IMBALANCE

Case	Parameter, dB	10 GHz	40 GHz	Slope, dB/GHz	Technological effects modeled
Strong coupling, rect. traces	|Scc21|	-3.359	-10.462	-0.2368	With ERD, no EP
		-2.307	-7.547	-0.1746	No ERD, with EP
		-3.415	-10.633	-0.2406	With ERD, with EP
	|Sdd21|	-3.767	-11.873	-0.2702	With ERD, no EP
		-2.764	-7.768	-0.1668	No ERD, with EP
		-4.275	-13.681	-0.3135	With ERD, with EP
	|Scd21|	-33.980	-31.258	+0.0907	With ERD, no EP
		-34.081	-28.472	+0.1869	No ERD, with EP
		-31.546	-30.474	+0.0357	With ERD, with EP
Weak coupling, rect. traces	|Scc21|	-3.631	-11.227	-0.2531	With ERD, no EP
		-2.567	-8.207	-0.1879	No ERD, with EP
		-3.781	-11.765	-0.2661	With ERD, with EP
	|Sdd21|	-3.374	-10.758	-0.2461	With ERD, no EP
		-2.548	-7.097	-0.1516	No ERD, with EP
		-3.730	-12.120	-0.277	With ERD, with EP
	|Scd21|	-35.894	-32.600	+0.1098	With ERD, no EP
		-31.859	-26.714	+0.1715	No ERD, with EP
		-31.121	-28.407	+0.0904	With ERD, with EP
Strong coupling, 60^0 traces	|Scc21|	-2.319	-8.924	-0.2202	With ERD, no EP
		-2.694	-8.184	-0.1830	No ERD, with EP
		-3.732	-11.760	-0.2676	With ERD, with EP
	|Sdd21|	-2.430	-9.635	-0.2401	With ERD, no EP
		-3.216	-8.905	-0.1896	No ERD, with EP
		-4.484	-14.642	-0.3385	With ERD, with EP
	|Scd21|	-33.831	-29.608	+0.1407	With ERD, no EP
		-34.789	-29.438	+0.1783	No ERD, with EP
		-39.747	-36.157	+0.1196	With ERD, with EP
Weak coupling, 60^0 traces	|Scc21|	-3.9292	-12.971	-0.3014	With ERD, no EP
		-3.0153	-8.926	-0.1970	No ERD, with EP
		-4.1203	-13.605	-0.3161	With ERD, with EP
	|Sdd21|	-3.650	-11.830	-0.2727	With ERD, no EP
		-2.919	-8.057	-0.1712	No ERD, with EP
		-4.071	-13.355	-0.3095	With ERD, with EP
	|Scd21|	-35.098	-31.950	0.1049	With ERD, no EP
		-34.609	-28.562	0.2016	No ERD, with EP
		-34.915	-33.119	0.0598	With ERD, with EP
Strong coupling, 45^0 traces	|Scc21|	-3.684	-11.553	-0.2622	With ERD, no EP
		-2.653	-8.161	-0.1836	No ERD, with EP
		-3.776	-11.869	-0.2698	With ERD, with EP
	|Sdd21|	-3.908	-12.542	-0.2878	With ERD, no EP
		-3.197	-8.9561	-0.1920	No ERD, with EP
		-4.487	-14.642	-0.3384	With ERD, with EP
	|Scd21|	-35.239	-32.587	+0.0884	With ERD, no EP
		-34.736	-29.462	+0.1756	No ERD, with EP
		-35.685	-34.571	+0.0371	With ERD, with EP
Weak coupling, 45^0 traces	|Scc21|	-4.095	-13.586	-0.3164	With ERD, no EP
		-2.913	-8.897	-0.1995	No ERD, with EP
		-4.311	-14.288	-0.3325	With ERD, with EP
	|Sdd21|	-3.782	-12.295	-0.2838	With ERD, no EP
		-2.912	-8.125	-0.1738	No ERD, with EP
		-4.210	-13.874	-0.3222	With ERD, with EP
	|Scd21|	-27.868	-26.424	+0.0482	With ERD, no EP
		-34.506	-28.613	+0.1964	No ERD, with EP
		-28.233	-27.759	+0.0158	With ERD, with EP

A. *Weak and Strong Coupling*

Fig. 10 and Table II show that the weak coupling results in the higher CM damping than the strong coupling, and that the sharper the trapezoid angle of the trace, the larger IL is experienced by the CM. The DM, on the contrary, is more damped at the strong coupling than at the weak one; the strong coupling for 45^0 and 60^0 cases provides the largest IL.

For the rectangular traces, mode conversion is almost unaffected by the strong/weak coupling. However, for the trapezoid cases, there is a significant difference between weak and strong coupling, especially for the 45^0 traces. This is due

to the stronger inhomogeneity of the fields around the trapezoid traces, and the rate of coupling affects CM and DM differently. Weak coupling for the 45^0 case produces the largest mode conversion, while the mode conversion in the strong-coupled 60^0 case is the lowest.

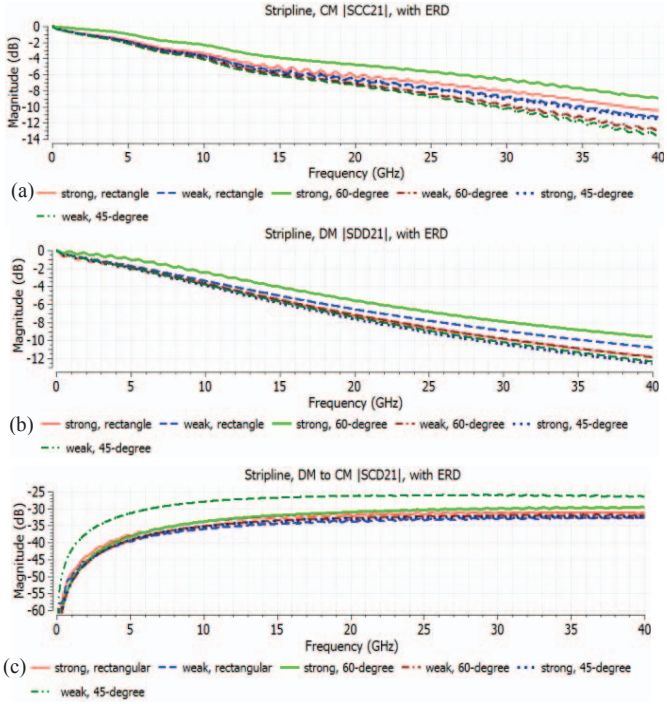

Fig. 10. CM $|S_{cc21}|$ (a), DM $|S_{dd21}|$ (b), and mode conversion $|S_{cd21}|=|S_{dc21}|$ (c) in strong and weak coupling cases in differential striplines. ERD is modeled.

B. *Effect of Epoxy Resin Pocket*

The results of modeling weak- and strong-coupled lines with EP and with/ without ERD are shown in Figs. 11-13 and Table II. The EP in both weak and strong coupling cases does not affect the CM propagation, since EP is located between the signal traces. However, its effect on the DM is significant, especially in the strong-coupled cases and with trapezoid traces as compared to the rectangular ones. The highest mode conversion is seen for 45^0 traces with ERD and weak coupling, independently of the epoxy pocket. The EP almost does not enhance mode conversion.

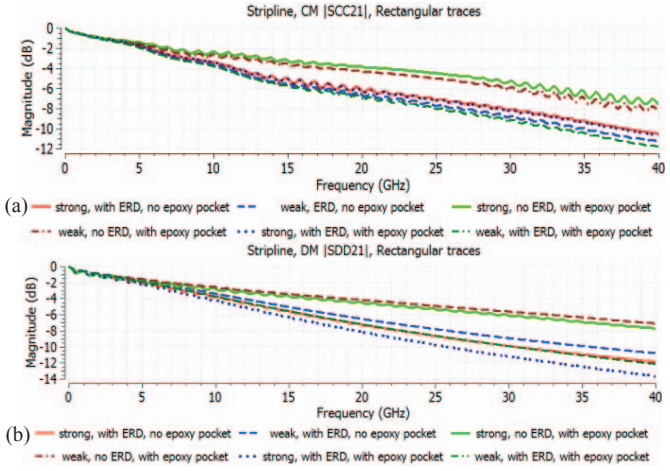

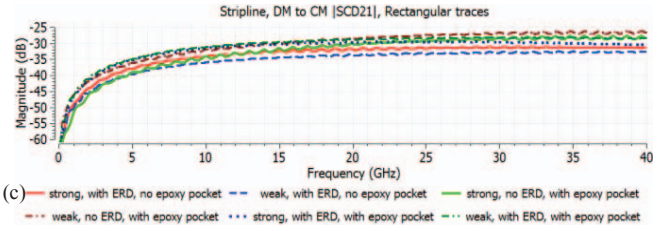

Fig. 11. CM $|S_{cc21}|$ (a), DM $|S_{dd21}|$ (b), and mode conversion $|S_{cd21}|=|S_{dc21}|$ (c) in strong- and weak-coupled striplines; with/without ERD; with/without EP. Rectangular traces and no roughness on the sides of the traces are modeled.

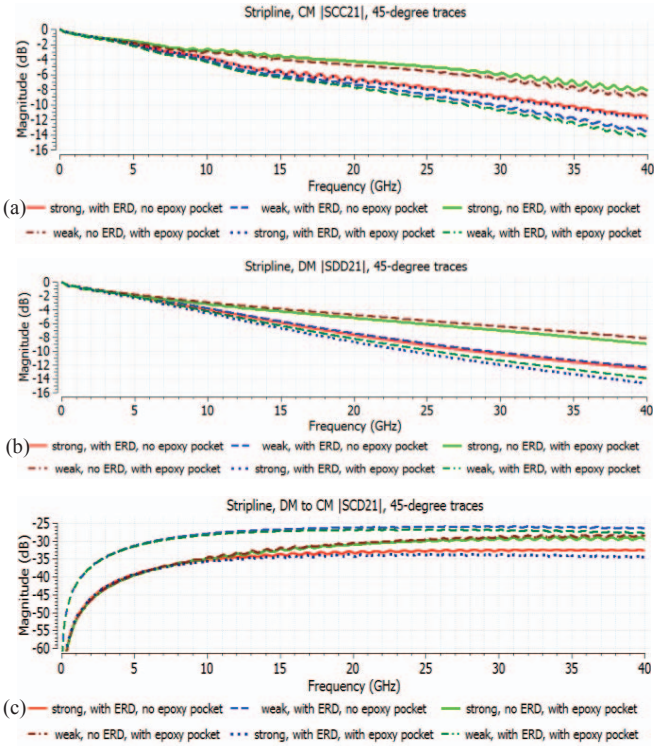

Fig. 12. CM $|S_{cc21}|$ (a), DM $|S_{dd21}|$ (b), and mode conversion $|S_{cd21}|=|S_{dc21}|$ (c) in strongly and weakly coupled differential striplines: with/without ERD and with/without epoxy pocket; 45^0 traces; no roughness on the sides of the traces.

Fig. 13 shows that the ERD on the sides of the traces (see Fig. 3) damps both CM and DM, and also reduces mode conversion for both strong and weak coupling.

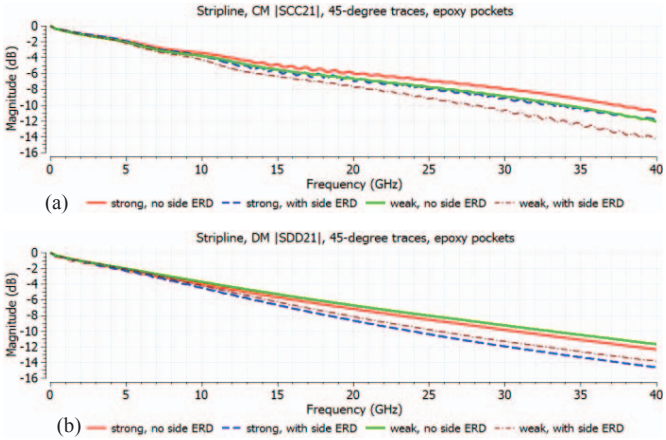

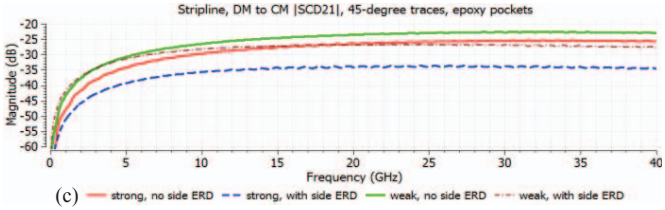

Fig. 13. CM $|S_{cc21}|$ (a), DM $|S_{dd21}|$ (b), and mode conversion $|S_{cd21}|=|S_{dc21}|$ (c) in strong and weak coupling cases in striplines. 45^0 traces; with epoxy pocket; with ERD under the traces, and with/without ERD on the sides of the traces.

C. *Effect of Differential Line Length*

The effect of the line length on weak and strong coupled imbalanced striplines was also studied. The 50-, 80-, and 100-mm lines imbalanced by 0.127 mm (5 mils) were modeled. The results are systematized in Table III, and also are shown in Fig. 14 (for the weak-coupled lines only). Herein, only traces of rectangular cross-section are presented.

TABLE III.
MIXED-MODE S-PARAMETERS AND SLOPES FOR STRIPLINE DIFFERENTIAL PAIRS WITH 5-MIL (0.127 MM) IMBALANCE AND DIFFERENT LINE LENGTHS

Case	Parameter, dB	10 GHz	40 GHz	Slope, dB/GHz	Technological effects modeled
Strong coupling, rect. traces, L=50 mm	|Scc21|	-1.890	-5.677	-0.1262	No ERD, with EP
		-2.141	-7.290	-0.1716	With ERD, with EP
	|Sdd21|	-1.923	-4.981	-0.1019	No ERD, with EP
		-2.801	-8.716	-0.1971	With ERD, with EP
	|Scd21|	-34.283	-25.903	+0.2793	No ERD, with EP
		-36.679	-30.268	+0.2137	With ERD, with EP
Strong coupling, rect. traces, L=80 mm	|Scc21|	-2.3073	-7.547	-0.1746	No ERD, with EP
		-3.415	-10.633	-0.2405	With ERD, with EP
	|Sdd21|	-2.764	-7.768	-0.1668	No ERD, with EP
		-4.275	-13.681	-0.3135	With ERD, with EP
	|Scd21|	-34.081	-28.472	+0.1870	No ERD, with EP
		-31.545	-30.474	+0.0357	With ERD, with EP
Strong coupling, rect. traces, L=100 mm	|Scc21|	-3.086	-9.461	-0.2125	No ERD, with EP
		-4.360	-13.845	-0.3161	With ERD, with EP
	|Sdd21|	-3.566	-9.750	-0.2061	No ERD, with EP
		-5.339	-16.953	-0.3871	With ERD, with EP
	|Scd21|	-35.565	-30.305	+0.1753	No ERD, with EP
		-35.202	-36.056	-0.0284	With ERD, with EP
Weak coupling, rect. traces, L=50 mm	|Scc21|	-2.059	-6.029	-0.1323	No ERD, with EP
		-2.364	-8.216	-0.1950	With ERD, with EP
	|Sdd21|	-1.639	-4.430	-0.0930	No ERD, with EP
		-2.349	-7.581	-0.1744	With ERD, with EP
	|Scd21|	-32.767	-24.758	+0.2669	No ERD, with EP
		-34.876	-29.014	+0.1953	With ERD, with EP
Weak coupling, rect. traces, L=80 mm	|Scc21|	-2.567	-8.207	-0.1879	No ERD, with EP
		-3.781	-11.765	-0.2661	With ERD, with EP
	|Sdd21|	-2.548	-7.097	-0.1516	No ERD, with EP
		-3.730	-12.12	-0.2797	With ERD, with EP
	|Scd21|	-31.859	-26.714	+0.1715	No ERD, with EP
		-31.121	-28.407	+0.0904	With ERD, with EP
Weak coupling, rect. traces, L=100 mm	|Scc21|	-3.579	-10.288	-0.2236	No ERD, with EP
		-4.859	-15.674	-0.3605	With ERD, with EP
	|Sdd21|	-3.174	-8.734	-0.1853	No ERD, with EP
		-4.639	-15.163	-0.3508	With ERD, with EP
	|Scd21|	-32.709	-28.180	+0.1509	No ERD, with EP
		-29.694	-28.919	+0.0258	With ERD, with EP

Obviously, the longer lines accumulate more IL for DM and CM. However, the mode conversion is larger for the longer lines, though the relative imbalance reduces. Slight reduction of mode conversion is also possible for the longer lines at the higher frequencies, since various losses, including dielectric, conductor, and foil roughness, increase with frequency.

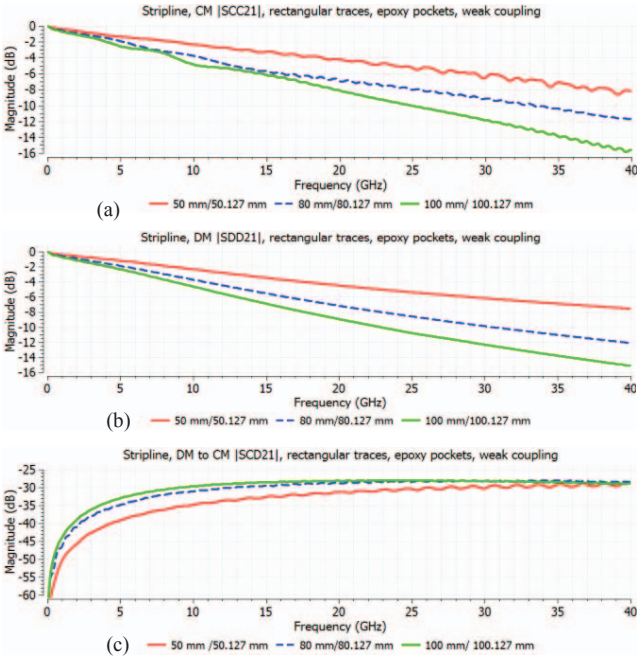

Fig. 14. CM $|S_{cc21}|$ (a), DM $|S_{dd21}|$ (b), and mode conversion $|S_{cd21}|=|S_{dc21}|$ (c) in weak-coupled striplines of different lengths, but the same imbalance (0.127 mm). Rectangular traces; with epoxy pocket; with ERD under the traces.

V. CONCLUSIONS

Weakly and strongly coupled imbalanced differential pairs, both microstrip and stripline show different behavior of mixed-mode S-parameters. For SI, weak coupling is preferable. However, this may be not the case for EMC. Mode conversion may be larger in the weak-coupled than in the strong-coupled cases, especially if the traces are trapezoid and other technological factors are considered. Copper foil roughness and epoxy-resin pocket between the traces may enhance the mode conversion. The most critical case for mode conversion enhancement is when there is weak coupling, 45^0 trapezoid traces, and significant roughness, especially at lower frequencies. Strong coupling usually results in mode conversion damping. Though the differences in slopes for the considered cases are just fractions of dB/GHz, as the line lengths and frequencies increase, these differences may become substantial.

REFERENCES

[1] B. Archambeault, J. C. Diepenbrock, and S. Connor, "EMI emissions from mismatches in high speed differential signal traces and cables", *IEEE Symp. EMC*, July 9-13, 2007, Honolulu, pp. 1-6.

[2] Y. Kayano, M. Ohkoshi, and H. Inoue, "Weak-coupled cross-sectional differential-paired lines with bend discontinuities for SI and EMI preformances", *EMC'14/Tokyo*, Japan, 2014, 13P1-B3, pp. 133-136.

[3] H. Johnson, *High Speed Signal Propagation: Advanced Black Magic*, Prentice Hall, 2003, pp. 389-396.

[4] M. Koledintseva, T. Vincent, and S. Radu, "Full-wave simulation of an imbalanced differential microstrip line with conductor surface roughness", *Proc. IEEE Symp. EMC&SI 2015*, Santa Clara, CA, 2015, pp. 34-39.

[5] CST STUDIO SUITE®, CST AG, Germany, www.cst.com.

[6] M. Koledintseva, T. Vincent, A. Ciccomancini, and S. Hinaga, "Method of effective roughness dielectric in a PCB: measurement and full-wave simulation verification", *IEEE Trans. Electromag. Compat.,* vol. 57, no. 4, pp. 807-814, 2015.